16th World Conference on Earthquake Engineering, 16WCEE 2017
Santiago Chile, January 9th to 13th 2017
Paper N° 4995
Registration Code: S-G1477881477

CASE HISTORIES OF GEOTECHNICAL ENGINEERING DAMAGE FROM THE 2016 M_W 6.0, M_W 6.2, and M_W 7.0 KUMAMOTO EARTHQUAKES

R. Kayen[1], S. Dashti[2], K.W. Franke[3], N. K. Oettle[4], B. Wham[5], T. Kokusho[6], H. Hazarika[7], & J. R. Calderon[8]

(1) Senior Scientist, USGS, Menlo Park, CA, USA & Adjunct Professor, UCLA, Los Angeles, CA, USA, rkayen@usgs.gov
(2) Assistant Professor, University of Colorado Boulder, Boulder, CO, USA, shideh.dashti@colorado.edu
(3) Assistant Professor, Brigham Young University, Provo, UT, USA, kfranke@et.byu.edu
(4) Senior Geotechnical Engineer, AECOM, San Jose, CA, USA, nicolas.oettle@aecom.com
(5) Postdoctoral Associate, Cornell University, Ithaca, NY, USA, bpw37@cornell.edu
(6) Professor, Civil Engineering Department, Chuo University, Tokyo, Japan, kokusho@civil.chuo-u.ac.jp
(7) Professor, Department of Civil & Structural Engineering, Kyushu University, Fukuoka, Japan, hazarika@civil.kyushu-u.ac.jp
(8) PhD Student, University of Colorado Boulder, Boulder, CO, USA, jenny.ramirezcalderon@colorado.edu

Abstract

The 2016 Kumamoto earthquakes are a series of events that began with an earthquake of moment magnitude 6.2 on the Hinagu Fault at 21:26 JST on April 14, 2016, at an epicentral depth of about 11 km. This event was followed by a larger moment magnitude 7.0 event on the Futagawa Fault, which struck at 01:25 JST on April 16, 2016 beneath Kumamoto City, Kumamoto Prefecture on Kyushu, Japan, at an epicentral depth of about 10 km. These events are the strongest earthquakes recorded in Kyushu during the modern instrumental era. The earthquake resulted in substantial damage to infrastructure, buildings, cultural heritage of Kumamoto castle, roads and highways, slopes, and river embankments due to earthquake-induced landsliding and debris flows. Surface fault rupture produced offset and damage to roads, buildings, river levees, an agricultural dam. Surprisingly, given the extremely intense earthquake motions, liquefaction-induced damage was mostly limited to a few districts of Kumamoto City and in the port areas, indicating that either the volcanic soils were largely unsusceptible to liquefaction or the presence of fines reduced the surficial manifestation of liquefaction and its effects, a significant finding from this event. The primary objective of this reconnaissance effort was the identification of important case histories for future investigations that help develop methodologies to mitigate damage in future earthquakes. Important individual case histories identified by the study are [1] fault rupture through the Oh-Kirihata Dam; [2] subsidence in the Aso Caldera Depression Zone; [3] fault rupture through the Shimojin-Cho River Canal; [4] and the surprising paucity of liquefaction and its effects.

.

Keywords: surface ruptures, earthquake reconnaissance, liquefaction, landslides, Caldera

1. Introduction

The Geotechnical Extreme Events Reconnaissance (GEER) Association, funded by the United States' National Science Foundation (US NSF), conducted a brief reconnaissance of the Kumamoto region following the April 16th M_W 7.0 earthquake (M_{JMA} 7.3) and the foreshocks of April 14th and 15th. The 2016 Kumamoto earthquakes are a series of earthquakes including a magnitude 7.0 mainshock, which struck at 01:25 JST on April 16, 2016 beneath Kumamoto City, Kumamoto Prefecture on Kyushu, Japan, at an epicentral depth of about 10 kilometers and a foreshock earthquake with a JMA magnitude 6.5 at 21:26 JST on April 14, 2016, at an epicentral depth of about 11 kilometers. Chain events of M_{JMA} 6.4 and 6.5 foreshocks followed by the M_{JMA} 7.3 mainshock that occurred within 28 hours, called the 2016 Kumamoto Earthquake, resulted in significant loss of life and properties. This was the strongest earthquake ever recorded in Kyushu (since the JMA was established). The epicenter of the main shock and the distribution of aftershocks are plotted on Fig. 1. More than 1,400 aftershocks have been recorded by the Meteorological Agency of Japan since April 14. The earthquake resulted in substantial damage to infrastructure including buildings, cultural heritage of Kumamoto castle, roads and highways, slopes and river embankment due to earthquake-induced landslides and debris flows, and fault-induced ground subsidence. At a surprisingly limited extent, liquefaction-induced damage was observed only in a few districts of Kumamoto City and in the port areas.

The Fire and Disaster Management Agency of Japan (FDMA) has reported that 50 people were killed (49 direct, 1 missing), 350 persons suffered severe injuries, and 1,234 suffered slight injuries. Property damage amounted to 2,487 houses completely destroyed, 3,483 houses partially destroyed, and 22,855 houses damaged but habitable. Fire destroyed 16 houses. In addition, about 3 billion USD has been estimated for the civil infrastructure losses. Reconstruction cost is estimated to be around 5-6 billion USD.

The authors conducted two surveys in the devastated areas: one during April 16-17, and the other during May 11-14, 2016 as part of the GEER team efforts to document the effects of the earthquakes (GEER Report, 2016). Five major case histories were identified as a part of the GEER reconnaissance. This report summarizes this earthquake sequence and these case histories.

2. Fault Mechanism

The 2016 Kumamoto mainshock was the strongest earthquake in Kyushu Island in the modern instrumental era. The fault rupture in the foreshocks and mainshock occurred along the Hinagu and Futagawa Faults. The Hinagu Fault is the southernmost fault in this area, just south of Kumamoto, and intersects the Futagawa Fault south of Kumamoto. The Futagawa Fault projects from that intersection point both to the west (the Uto Segment) and to the northeast (the Futagawa Segment). Each of these faults was, in general, previously mapped by the Geological Society of Japan prior to these earthquakes. See (Figure 1, GSJ 2016) for a depiction of the faults.

Sources vary as to whether the foreshocks ruptured the ground surface, but if they did, it would have been on the Hinagu Fault. In the mainshock, both faults and both segments of the Futagawa Fault appear to have ruptured, although most of the rupture and the largest surface displacements were on the Futagawa Segment of the Futagawa Fault. In total, about 28 km of the Futagawa Fault and 8 km of the Hinagu Fault experienced surface fault rupture (GSJ 2016).

3. Geology of the Kumamoto Area

The Kumamoto-Aso San region of Kyushu Island is a complex structure of Paleozoic and Mesozoic rocks associated with Island arc plutonism/volcanism, accretionary tectonics metamorphism, and the filling of backarc and forearc basin. The Geologic Survey of Japan has published a map of the Kumamoto Quadrange (GSJ, AIST, 2004, NI-52-11 in Japanese) that shows this complex structure of Paleozoic, Mesozoic, Cenozoic, and Neogene rocks. Of the Paleozoic, Kyushu is underlain by a suite of arc-tectonics-related igneous and metamorphic terrain including the mafic/ultramafic Permian Yamaga Metagabbro, Late Permian Mizukoshi Formation, and the Mississippian & Pennsylvanian to Permian Sangun-Renge Metamorphic Rocks.

Mesozoic structures also indicate arc-volcanism with preservation of more felsic igneous rocks than preserved from the Paleozoic and arc-sedimentary basin structures including the Triassic-to-Jurassic Suō Metamorphic Rocks, the Cretaceous Higo Metamorphic Rocks, the Cretaceous marine and non-marine sedimentary of the Mifune and Himenoura Groups, and Cretaceous granitic rocks.

Paleocene, Neogene and Quaternary rocks are associated with arc-volcanics and sedimentary structures shed from these volcanic rocks including Miocene basalts and andesites, Pliocene basalts, andesites, and rhyolites. Significant volumes of Quaternary volcanic sources include the Unzen crater, Aso San Caldera, and the Mt. Kimbo and Mt. Tara volcanoes. Eocene to Oligocene sedimentary rocks are Ginsui and Hokonoko Formations, Ōmuta, Isahaya, Manda, Ochi and Kishima Groups. Neogene Quaternary volcanoclastic sediment forms the Kumamoto basin and Shimabara Bay depocenter.

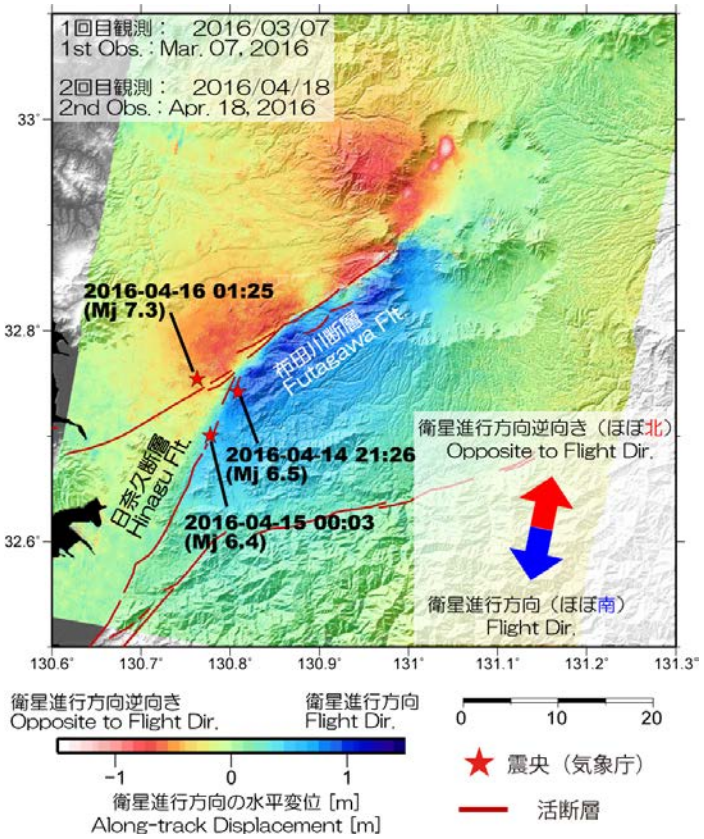

Fig. 1. Multiple Aperture Interferometry (MAI) processed from ALOS-2 provided by the Geospatial Information Authority of Japan (GSI). The red lines are previously mapped active fault traces.

4. Seismicity

Two strong foreshocks (Moment magnitude M_w 6.0 and 6.2) on April 14th and a mainshock (Mw 7.0) on April 15th, 2016 caused strong levels of shaking in the region, damaging buildings and other infrastructure. During the M6.5 foreshock, the largest recorded ground acceleration of 1.6g was measured at Mashiki Town. During the mainshock, the peak ground accelerations again exceeded 1g at Mashiki Town. These earthquakes were shallow (hypocentral distances of approximately 11 km and 12 km, respectively, according to the Japan Meteorological Agency) under the City of Kumamoto. Building collapse due to strong shaking and landslides as well as damage to roads and lifelines were observed. Figure 2 shows the distribution of PGA and PGVs recorded during the mainshock (Goto 2016).

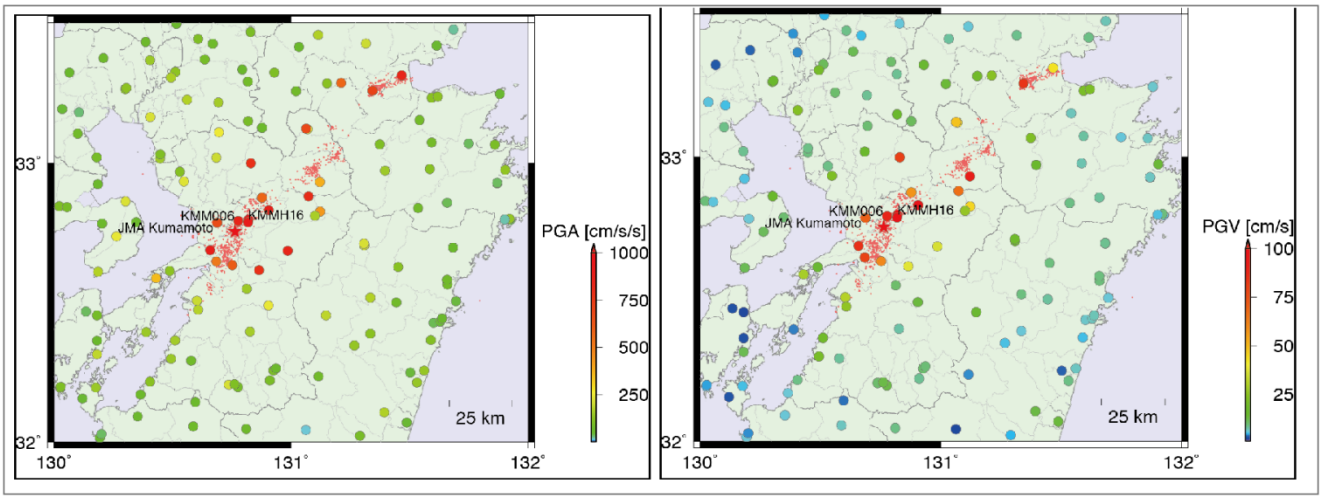

Fig. 2. Distribution of PGAs and PGVs recorded during the main M 7.0 earthquake (Goto 2016).

5. Landslides

Widespread landsliding was caused by the Kumamoto Earthquakes in the steep volcanic geology of the region. Several hundred landslides are believed to have occurred based on satellite imagery interpretation conducted by the Geospatial Information Authority of Japan (Fig. 3). The GEER reconnaissance team observed numerous landslides while driving through the region.

The native slopes in the area are composed of various types of volcanic deposits. These deposits, in general, are very susceptible to weathering and subsequent landsliding. Landslides in these formations are common around the region, and throughout Japan, and have been triggered by both intense rain and seismic events (Wang et al. 2006, Jitousono et al. 2008, Sidle and Chigira 2004, Yamao et al. 2016).

The Great Aso Landslide was likely the largest landslide that occurred as a result of the Kumamoto Earthquakes. The head scarp of the landslide was approximately 350 m higher in elevation than a canyon that ran directly beneath the landslide area. The horizontal distance from the head scarp to the canyon was approximately 700 m (Fig. 4). A bridge previously crossed the canyon directly beneath the landslide, but was destroyed in the earthquake, presumably by this landslide. The remnant of one of the abutments is visible. There was also significant slope failure of the canyon wall slopes throughout this area, independent of the overlying Great Aso Landslide. The Great Aso Landslide source area is mapped as Pyroxene Andesite Lava, lava flow and dike (Pa) in a 1:50,000 “Geological Map of Aso Volcano”.

Extensive UAV video of the landslide and the surrounding area is publically available on the Geospatial Information Authority of Japan website (http://maps.gsi.go.jp/overlay/160414kumamoto/uav/20160416uav01.wmv), and a digital elevation model of the landslide has been produced by the Japan Asia Group (http://www.kkc.co.jp/service/bousai/csr/disaster/201604_kumamoto/index.html).

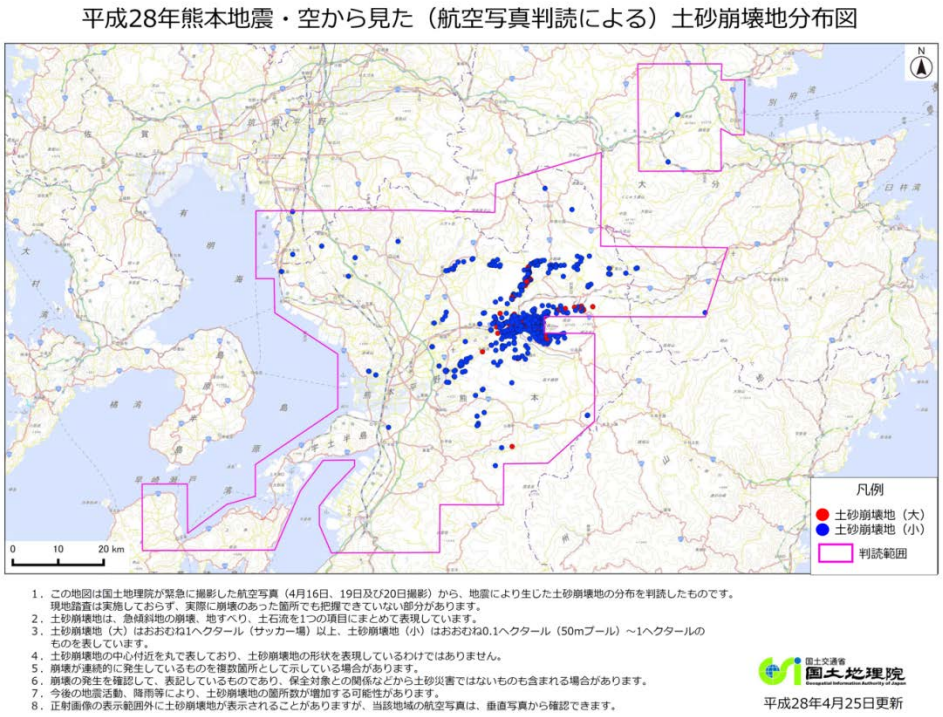

Fig. 3. Overview of landslides from the Kumamoto Earthquakes produced by the Geospatial Information Authority of Japan (GSI).

Fig. 4. Front view of the Great Aso Landslide that likely destroyed a bridge, the remnant abutment of which is visible on the left side of the photo.

6. Oh-Kirihata Dam

The Futagawa fault ruptured through an approximately 0.5 km long by 0.25 km wide water reservoir. The fault rupture passed through the western flank of the reservoir and through the main spillway. No catastrophic release of water occurred. However, the reservoir experienced significant damage, both as a result of the surface fault rupture and as a result of the strong ground motions. This presents a valuable case history of the response of dams to surface fault rupture.

GEER made extensive terrestrial LiDAR, UAV, photographic, and manual surveys of the reservoir to record the damage caused by the earthquake. The reservoir was almost fully drawn down at the time of GEER's reconnaissance, with only minor emergency repair work done, so the GEER team had extensive access to the reservoir to record damage.

GEER is currently working on developing three-dimensional models of the reservoir, dam, and spillway to fully document the condition of the reservoir after the earthquake. A view of the spillway from the UAV-generated 3D model is provided in Fig 5. An interactive 3D model is available online at: http://prismweb.groups.et.byu.net/JD/App/.

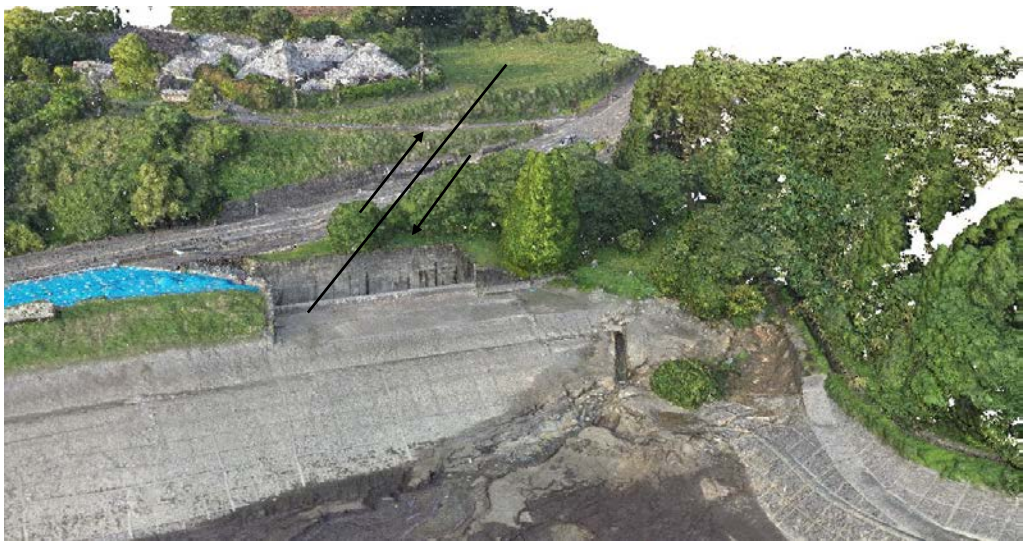

Fig.5 Three-dimensional (3D) model of the spillway generated by UAV data.

7. Aso Caldera Depression Zone

In the Aso Caldera, an approximately 10 km long "zone of depression" resulted from the Kumamoto earthquake mainshock. The zone of depression was typically 30 m to 110 m wide with roughly vertical offsets on each side of the depression zone of about 0.5 m to 2.5 m with a minor strike-slip component. The cause of the zone of depression is of interest. Potential causes include liquefaction, earth compaction, lateral spreading, and fault rupture (Figure 6). Lin et al. (2016) postulate that the depression zone is actually a graben formed by co-seismic rupture of two normal faults within the Aso caldera.

The GEER team made extensive UAV flights over approximately 4 km of the depression zone to create a large, unique three-dimensional (3D) model of the ground deformations. Extensive terrestrial LiDAR data was also acquired over a large portion of the depression zone where a bridge crossed the depression. Extensive photographing and manual mapping of the deformation was also completed by GEER. A composite overview of the entire UAV-generated preliminary 3D model is presented in Fig. 6. A preliminary, interactive 3D model of a residential house that was located immediately on the hanging wall of the depression zone is available at: http://prismweb.groups.et.byu.net/JH/App/.

Fig. 6 Portion of the depression zone shown in the 3D point cloud model developed from UAV.

8. Shimojin-Cho River Canal

A unique aspect of the 2016 Kumamoto Earthquake is the availability of pre- and post-mainshock aerial LiDAR. Asia Air Survey conducted a detailed aerial LiDAR survey shortly after the initial foreshock of much of the Futagawa and Hinagu faults. After the mainshock occurred, these aerial surveys were performed again, making the generation of a detailed earthquake-induced displacement model possible. In addition, the Geospatial Information Authority of Japan (GSI) also conducted an aerial LiDAR survey of an even greater zone in 2005 from which comparisons can be made.

Because this LiDAR data represents a relatively unique dataset for analyzing ground deformation resulting from surface fault rupture, GEER visited a number of sites in the aerial LiDAR coverage zone. Of particular interest was a location where the Futagawa fault crossed a canal embankment. The response of the embankment to underlying fault rupture might be useful for studies on the performance of levees, dams, and other earth structures subjected to surface fault rupture. GEER therefore conducted a detailed terrestrial LiDAR scan of this area to compare again the aerial LiDAR data (Fig. 7)

Although the canal was not full of water at the time of the earthquake, the damage observed by GEER was relatively minor, despite measured fault displacements of about 57 cm horizontal and 28 cm vertical. A second, conjugate fault, with opposite direction strike-slip motion, also happened to cross the canal embankment at roughly the same location, making the deformation field relatively complex. The estimated displacement on this fault was about 29 cm horizontal and 13 cm vertical.

9. Paucity of Liquefaction

One of the striking features of this earthquake was the relatively low number of liquefaction sites observed given the extremely strong ground motions recorded throughout the Kumamoto region and the large areas mapped as young alluvial deposits. GEER did visit a number of sites where liquefaction was observed, and other reconnaissance teams also observed a number of areas of liquefaction (shown in Figure 8). However, much more liquefaction-induced damage was expected based on the team's experience documenting liquefaction after earthquakes of such intensity in alluvial deltaic areas. A detailed map of liquefaction-related damage to building structures observed by GEER is provided in Fig.8 in addition to a picture of one example building affected by liquefaction.

It is of interest to determine the specific reasons why more liquefaction did not occur or why surficial evidence of liquefaction and its effects on structures was limited. Given the high intensity of shaking, the relatively high ground water levels, and the abundant presence of loose granular soils with low SPT blow counts as evident in a number of Geotechnical reports in the area, reasons for limited evidence of liquefaction may be attributed to the

presence of plastic (non-susceptible) soils within or between layers of loose sand, age of the soil deposit, and volcanic geologic origin of the sediments. The GEER team expects that the soil plasticity, resulting from the volcanic origin of the sediments, is the most likely cause. The authors recommend that further studies (e.g., soil borings, laboratory testing, and extensive in-situ testing) be conducted at liquefaction and particularly non-liquefaction sites, where liquefaction would otherwise have been expected, to determine the causes of limited liquefaction evidence and effects resulting from the Kumamoto Earthquakes.

Fig.7 The terrestrial LiDAR setup and damage to the canal embankments. The main fault crossing is at the location of the repairs visible in the photograph.

In addition to liquefaction effects on structures, the team was interested in identifying cases where lateral spreading occurred and cases where lateral spreading was expected but did not occur (i.e., zero-displacement lateral spread). Remarkably, only one significant liquefaction-related lateral spread was encountered by the GEER team during the Kumamoto reconnaissance mission. This lateral spread was located in Akisumachi Nuyamazu, adjacent to a pipeline bridge and traffic bridge along route 232 crossing a tributary of the Midorikawa River at the east of Kumamoto City limits (32.77369° N 130.78384° E). A least seven repairs to water distribution pipelines in the immediate area were required, including three ruptures of the 800-mm-diameter steel transmission main crossing the river.

A LIDAR scan was taken at the north side of field exhibiting largest ground cracking (Figure 9). This area was boarded by a concrete lined drainage canal to the north, and the river to the south. Based on observations, including limited damage to the drainage canal at the north, the team believes the majority of movement was south toward the river. In the residential area north of the small canal, several extension features were observed in sidewalk blocks and around buildings, indicating a slight movement of this area toward the river.

West of the LIDAR scan extension cracks propagated through a one-story concrete block structure resulting in greater than 0.5 m of relative wall displacement. Evidence of surface cracking was observed in the field to the west of this structure, generally oriented parallel to the river. Large road patches were also observed to the west along the river frontage road, likely repairs of lateral spreading. The extent of observable ground cracking to the west was within 100 m of the LIDAR scan.

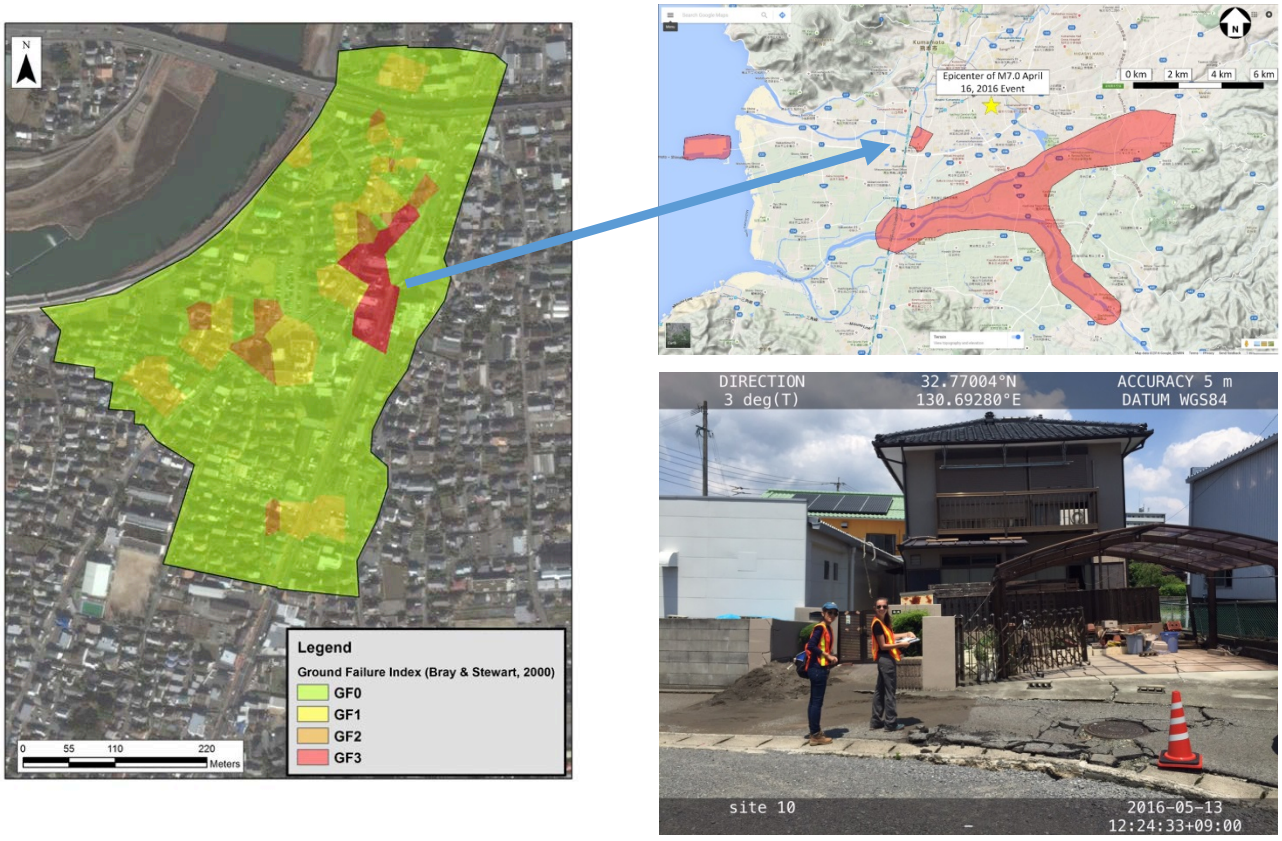

Fig.8 Maps produced by GEER of observed liquefaction and related damages in the Kumamoto region and picture of building settlement and tilt due to soil liquefaction in the south-east corner of the Shirakawa River (building settlement with respect to the surrounding ground in the order of 10 cm and tilt of 2 degrees).

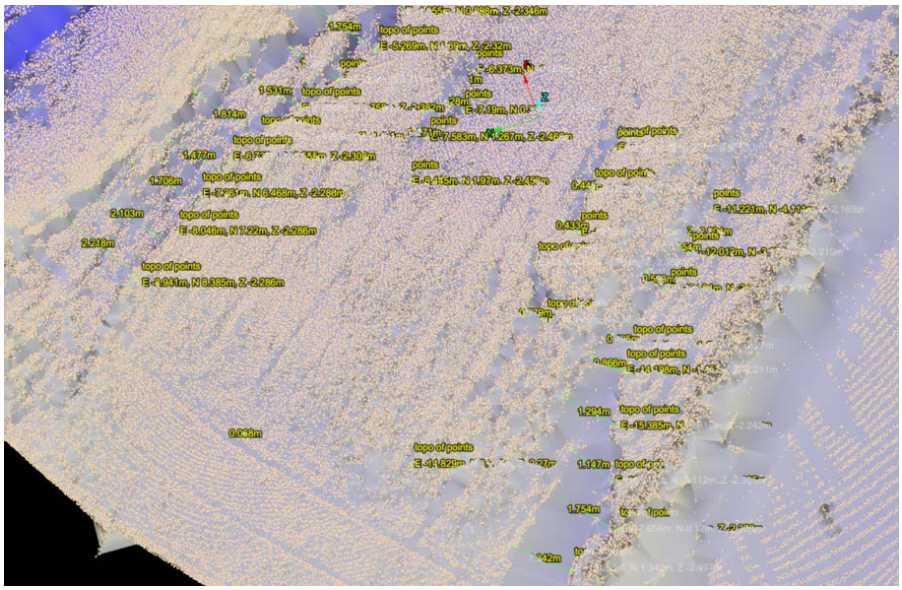

Fig.9. Measurements of lateral spread elevations and fissure locations from LIDAR data at Mashiki town.

10. Conclusions

These four case histories documented by GEER will provide valuable insights for the performance of engineered structures and systems during strong earthquake shaking. We recommend that future studies be conducted to evaluate in more detail the specific causes and effects of each case history. It is the mission of GEER to quickly gather the perishable data documenting the damage that occurred and make measurements of that damage before significant repair work removes evidence of damage. We hope that the information gathered by this GEER team serves to further research into the response of infrastructure during strong earthquakes and other natural hazards.

11. Acknowledgments

The work of the GEER Association, in general, is based upon work supported in part by the National Science Foundation through the Geotechnical Engineering Program under Grant No. CMMI-1266418. The GEER Association is made possible by the vision and support of the NSF Geotechnical Engineering Program Directors: Dr. Richard Fragaszy and the late Dr. Cliff Astill. GEER members also donate their time, talent, and resources to collect time-sensitive field observations of the effects of extreme events.

12. References

Hoshizumi, H., Ozaki, M., Miyazaki, K., Matsuura, H., Toshimitsu, S., Uto, K., Uchiumi, S., Komazawa, M., Hiroshima, T., and Sudo, S. (2004). *Geological Map of Japan 1:200,000, Kumamoto.* Geological Survey of Japan, AIST.

Goto, H. (2016). 2016 Kumamoto Earthquake. Report submitted to DPRI, Kyoto University, Japan.

GSI (2016). "平成２８年熊本地震に関する情報". Geospatial Information Authority of Japan, http://www.gsi.go.jp/BOUSAI/H27-kumamoto-earthquake-index.html (retrieved: 05/28/2016).

Japanese Geotechnical Society, (2016). "Disaster report of the 2016 Kumamoto earthquake" [preliminary report] (地盤工学会 平成28年熊本地震 災害報告[速報版])", https://www.jiban.or.jp/images/somufile/H28kumamoto_%20jishinsaigai_sokuho20160418-3.pdf (retrieved: 05/26/2016).

Kayen, R., Dashti, S., Kokusho, T., Hazarika, H., Franke, K., Oettle, N.K., Wham, B., Calderon, J.R., Briggs, D., Guillies, S., Cheng, K., Tanoue, Y., Takematsu, K., Matsumoto, D., Morinaga, T., Furuichi, H., Kitano, Y., Tajiri, M., Chaudhary, B., Nishimura, K., Chu, C. : Geotechnical Aspects of the 2016 MW 6.2, MW 6.0, and MW 7.0 Kumamoto Earthquakes, *Geotechnical Extreme Events Reconnaissance (GEER) Association*, Report Number GEER-048, 2016.

Konagai, K., Kiyota, T., Shiga, M., Tomita, H., Okuda, H., and Kajihara, K. : Ground fissures that appeared in Aso Caldera Basin in the 2016 Kumamoto Earthquake, Japan, *JSCE Journal of Disaster FactSheets*, FS2016-E-0003, 2016.

Lin, A., Satsukawa, T., Wang, M., Mohammadi Asl, Z., Fueta, R., and Nakajima, F. (2016). Coseismic rupturing stopped by Aso volcano during the 2016 M_w7.1 Kumamoto earthquake, Japan. *Science,* 20 Oct. 2016. DOI: 10.1126/science.aah4629.